(9) M. Calligaris, C. Nardin, L. Randaccio, and C. Tauzher, *Inorg. Nucl. Chem. Lett.*, **9**, 419 (1973).

(10) B. C. Wang and W. P. Schaefer, *Science*, **166**, 1404 (1969).

(11) M. Calligaris, G. Nardin, L. Randaccio, and A. Ripamonti, *J. Chem. Soc. A*, 1069 (1970).

(12) L. A. Lindblom, W. P. Schaefer, and R. E. Marsh, *Acta Crystallogr., Sect. B*, **27**, 1461 (1971).

(13) No assumption about the formal oxidation states of either the cobalt atoms or the dioxygen ligand is implied by the name.

(14) W. P. Schaefer and R. E. Marsh, *Acta Crystallogr., Sect. B*, **25**, 1675 (1969).

(15) With the exception of C. K. Johnson's ORTEP program, the computer programs used were from Caltech's CRYM system: D. J. Duchamp, Abstacts, American Crystallographic Association Annual Meeting, Bozeman, Mont., 1964, Paper B14.

(16) S. W. Peterson and H. A. Levy, *Acta Crystallogr.*, **10**, 70 (1957).

(17) F. L. Hirshfeld and D. Rabinovich *Acta Crystallogr., Sect. A*, **29**, 510 (1973).

(18) (a) The function minimized was $S = \sum w(F_o^2 - F_c^2)^2$, where F_o^2 and F_c^2 are the observed and calculated structure factor square amplitudes and the weights w are taken as $1/\sigma^2(F_o^2)$. Neutral atom scattering factors were used for all the atoms.[18b,c] The real component of anomalous dispersion for cobalt atoms was included (interpolated as −2.19 electrons using Cromer's compilations[18d]). (b) "International Tables for X-Ray Crystallography", Vol. III, Kynoch Press, Birmingham, England, 1968, p 204. (c) R. F. Stewart, E. R. Davidson, and W. T. Simpson, *J. Chem. Phys.*, **42**, 3175 (1965). (d) D. T. Cromer, *Acta Crystallogr.*, **18**, 17 (1965).

(19) One block contained the coordinates while the thermal parameters along with the scale factor were divided between two other blocks in the 505-parameter refinement. The parameters of the solvent atoms were generally kept fixed during the main refinements. The total number of parameters, including the dependent ones, was 814.

(20) Two particularly troublesome reflections were the intense F_{002} and F_{020}. In the two- and three-orientation solvent models, the former was calculated some 50–100 electrons too high, while the latter was calculated about 80 electrons too low. This trend, also present in many other strong reflections, could be interpreted to mean that the solvent region was electron density deficient, since the two reflections above are proportional to cos $4\pi z$ and cos $4\pi y$ and the solvent molecule has the coordinate ranges $y = 0.43 \pm 0.06$ and $z = 0.26 \pm 0.04$. Since the z coordinate of one of the cobalt atoms is 0.52, the solvent region deficiency may have been compensated by the distortion of the cobalt thermal parameters. The sum of this and other smaller effects apparently resulted in the drastically distorted structure referred to as model A.

(21) The population factors were determined by comparing the magnitudes of the residual density peaks in the difference map, guided by the assumption that the thermal parameters of the two solvent molecules were approximately the same. The bond distances and angles were loosely constrained to be the expected ideal values.

(22) S. C. Abrahams and E. T. Keve, *Acta Crystallogr., Sect. A*, **27**, 157 (1971).

(23) A. Avdeef and W. P. Schaefer, to be submitted for publication.

(24) Supplementary material.

(25) (a) The agreement factors used in Table II are based on deviations of F^2 from the corresponding weighted means of groups of duplicated reflections. The individual-octant factors are defined as $R^i = \sum_n^{N_i}|\Delta_{ni}|/\sum \bar{F}_n^2$, $R_w^i = [(\sum \sigma_{ni}^2/\sigma_{ni}^2)/(\sum \bar{F}_n^4/\sigma_{ni}^2)]^{1/2}$, and the goodness of fit, $\mathrm{GOF}^i = [N_i^{-1} \sum \Delta_{ni}^2/\sigma^2(\Delta_{ni})]^{1/2}$, where $\Delta_{ni} = F_{ni}^2 - \bar{F}_n^2$, $\sigma^2(\Delta_{ni}) = \sigma_{ni}^2 - 1/\sum_m(1/\sigma_{nm}^2)$, $\bar{F}_n^2$ is the nth weighted mean (interoctant) structure factor square amplitude, and N_i is the number of reflections in the ith octant which have duplicates in other octants. The overall (mean) agreement indices are defined as $R = \sum_n^N \sum_m^{M_n} |\Delta_{nm}|/\sum\sum F_{nm}^2$, $R_w = [(\sum\sum \Delta_{nm}^2/\sigma_{nm}^2)/(\sum\sum F_{nm}^4/\sigma_{nm}^2)]^{1/2}$, and $\mathrm{GOF} = [N^{-1} \sum_n (M_n - 1)^{-1} \sum_m \Delta_{nm}^2/\sigma_{nm}^2]^{1/2}$, where N is the number of duplicate sets and M_n is the number of reflections in the nth set of duplicates. (b) The agreement factors (cf. ref 18a) reported for the model refinement are goodness of fit, $\mathrm{GOF} = [S/(N_o - N_p)]^{1/2}$, where $N_o = 5314$ reflections and $N_p = 543$ independent parameters, $R_F = \sum||F_o| - |F_c||/\sum|F_o|$, $R_{wF} = [(\sum wF_o^2(|F_o| - |F_c|)^2)/(\sum wF_o^4)]^{1/2}$, and $R_{wF^2} = [S/\sum wF_o^4]^{1/2}$.

(26) Since a satisfactory weighting scheme was obtained from the merging of duplicate reflections, it did not seem justifiable to change the weighting scheme as a result of biases which were probably model based rather than data based.

(27) L. Pauling, "The Nature of the Chemical Bond", 3rd ed, Cornell University Press, Ithaca, N.Y., 1960, pp 351–352.

(28) The estimated standard deviations are based on isotropic coordinate errors and thus do not incorporate correlation effects.

(29) W. C. Hamilton, "Statistics in Physical Sciences", Ronald Press, New York, N.Y., 1964, Chapter 3.

(30) F. R. Fronczek, W. P. Schaefer, and R. E. Marsh, *Inorg. Chem.*, **14**, 611 (1975).

(31) F. R. Fronczek and W. P. Schaefer, *Inorg. Chim. Acta*. **9**, 143 (1974).

(32) R. E. Marsh and W. P. Schaefer, *Acta. Crystallogr., Sect. B*, **24**, 246 (1968).

(33) W. P. Schaefer and R. E. Marsh, *J. Am. Chem. Soc.*, **88**, 178 (1966); *Acta Crystallogr.*, **21**, 735 (1966).

(34) W. P. Schaefer, *Inorg. Chem.*, **7**, 725 (1968).

(35) F. R. Fronczek, W. P. Schaefer, and R. E. Marsh, *Acta Crystallogr., Sect B*, **30**, 117 (1974).

(36) J. R. Fritch, G. G. Christoph, and W. P. Schaefer, *Inorg. Chem.*, **12**, 2170 (1973).

(37) T. Shibahara, S. Koda, and M. Mori, *Bull. Chem. Soc. Jpn.*, **46**, 2070 (1973).

(38) U. Thewalt and R. E. Marsh, *J. Am. Chem. Soc.*, **89**, 6364 (1967); *Inorg. Chem.*, **11**, 351 (1972).

(39) G. G. Christoph, R. E. Marsh, and W. P. Schaefer, *Inorg. Chem.*, **8**, 291 (1969).

(40) C. Floriani and F. Calderazzo, *J. Chem. Soc. A*, 946 (1969).

(41) M. Calligaris, G. Nardin, and L. Randaccio, *Coord. Chem. Rev.*, **7**, 385 (1972).

(42) The first value in the brackets refers to the internally determined[43] estimated standard deviation in the least significant digit, while the second value refers to the externally determined error.

(43) W. C. Hamilton and S. C. Abrahams, *Acta Crystallogr., Sect. A*, **26**, 18 (1970).

(44) W. R. Scheidt, J. A. Cunningham, and J. L. Hoard, *J. Am. Chem. Soc.*, **95**, 8289 (1973).

(45) W. R. Scheidt, *J. Am. Chem. Soc.*, **96**, 84 (1974).

(46) V. Schomaker and K. N. Trueblood, *Acta Crystallogr., Sect. B*, **24**, 63 (1968).

(47) W. C. Hamilton and J. A. Ibers, "Hydrogen Bonding in Solids", W. A. Benjamin, New York, N.Y., 1968, p 16.

(48) Oxygen loss accounts for only 3.5% of the weight of the dimer. Yet the first observed weight loss in the thermogram is 17%, followed by an additional loss of 8% under 140 °C. The weight loss associated with the oxygen, the solvent, and one of the coordinated piperidine molecules is 20% and may explain the first observed loss. The loss of the other piperidine accounts for an additional 9%.

Contribution from the "Laboratoire de Chimie du Solide du CNRS",
Université de Bordeaux I, 33405 Talence, France

Crystal Structure of Sodium Lanthanum Orthovanadate, $Na_3La(VO_4)_2$

M. VLASSE,* R. SALMON, and C. PARENT

Received December 2, 1975 AIC508670

The crystal structure of sodium lanthanum orthovanadate has been determined and refined by full-matrix least-squares methods using automatic diffractometer data to a residual $R = 0.081$. The space group is $Pbc2_1$ ($Pca2_1$) with $a = 5.582$ (2) Å, $b = 14.240$ (8) Å, and $c = 19.420$ (9) Å. The structure is made up of isolated VO_4 tetrahedra and of sodium and lanthanum atoms arranged in an ordered way. A description of the structure from a topological viewpoint has been given.

Introduction

Rare earth orthovanadates of formula $LnVO_4$ crystallize with the tetragonal zircon-type structure,[1,2] with the exception of $LaVO_4$ which has a monazite-type structure. They make up a unique series for the study of the relationships between structure and physical properties.

Since some of these compounds have interesting optical properties which seem to be related to the position of the Ln^{3+}

ion in a tetrahedral VO_4^{3-} network,[3] we believed it appropriate to investigate other rare earth vanadate systems. To this end, a study was undertaken on compounds with a general formula $Na_3Ln(VO_4)_2$.

The only previous work in this field was a crystal chemical study on the system Na_3VO_4–$LaVO_4$ between 650 and 1200 °C.[4] The $Na_3La(VO_4)_2$ phase was isolated, but due to the complexity of its powder diffraction pattern no precise crystallographic data were obtained. Recently Salmon et al.[5] have isolated a series of double orthophosphates $Na_3Ln(PO_4)_2$ where Ln is a rare earth, except Tm, Yb, and Lu. These compounds are found to be isotypic with $Na_3La(VO_4)_2$. On this basis it seemed worthwhile to prepare single crystals of this phase and to carry out a complete crystallographic study.

Experimental Section

Preparation and Crystal Growth. The orthovanadate $Na_3La(VO_4)_2$ was prepared in powder form from a stoichiometric mixture of Na_3VO_4 and $LaVO_4$ heated first at 850 °C for 15 h and then at 1050 °C for 4 days.

Single crystals of $Na_3La(VO_4)_2$ were grown from a sodium orthovanadate flux containing 5 mol of Na_3VO_4 and 2 mol of $Na_3La(VO_4)_2$, in a platinum crucible kept at 1050 °C for 15 h and then cooled to 700 °C at a rate of 4 deg/h. The colorless single crystals in the form of rectangular blocks were separated from the solid flux by repeated washing in hot water.[5] The powder pattern of the single crystals was found to be identical with that of the polycrystalline samples.

X-Ray Diffraction Data. The single-crystal diffraction data from zero and upper-layer Weissenberg and precession photographs indicate an orthorhombic Laue symmetry *mmm*. The systematic extinctions $0kl$, $k = 2n + 1$, and $h0l$, $l = 2n + 1$, are consistent with the space group $Pbc2_1$ (C^5_{2v}) or $Pbcm$ (D^{11}_{2h}). The cell dimensions obtained and refined from single-crystal data are $a = 5.582$ (5) Å, $b = 14.240$ (8) Å, and $c = 19.420$ (9) Å. The reported error for the parameters represents the average deviation in the observed cell constants. The measured density, $d_{\text{exptl}} = 3.76$ (1) g/cm^3, indicates a cell containing eight formula units ($d_{\text{calcd}} = 3.79$ g/cm^3).

A single crystal of $Na_3La(VO_4)_2$ of rectangular form and 0.17 × 0.15 × 0.09 mm^3 in size was mounted about its *a* axis. The intensity data were collected on an Enraf-Nonius CAD3 three-circle automatic diffractometer using Mo Kα radiation with a pyrolytic graphite monochromator (002) and a 4° takeoff angle. A scintillation counter and a θ–2θ multiple scanning technique with a scan rate of 10° (2θ)/min was used. The background was taken at each end of the scanned range for a time equal to the actual scan time. Three control reflections measured for every batch of 50 reflections showed a random fluctuation of about 4%. A total of 3350 independent reflections were measured to a value of $2\theta_{\max} = 70°$. Of these, 2844 had intensity greater than $3\sigma(I)$ where $\sigma(I) = [\text{total counts} + \text{background counts}]^{1/2}$ and were considered to be observed. The total scan count (I_m) and the background counts (I_l, I_r) were combined to yield a set of integrated intensities by the relationship $I_o = I_m - (I_l + I_r)$. These intensities were corrected for Lorentz and polarization effects but not for absorption ($\mu r_{\max} = 0.69$).

Solution and Refinement of the Structure. A three-dimensional Patterson synthesis was calculated and an attempt to solve the Patterson in the centrosymmetric space group was made. This attempt was not successful.

This failure is corroborated by the lack of peak concentration on the Harker line $00w$ and the presence of a considerable concentration of peaks on the Harker plane $u, v, {}^1/_2$ indicating that $Pbc2_1$ ($Pca2_1$) is the most probable space group. The structure was finally solved in this space group. The position of the six heavy atoms was determined from the La–La and La–V vectors. Difference Fourier maps were used to locate the 6 sodium and 16 oxygen atoms. A number of cycles of block-diagonal and full-matrix least-squares refinements reduced the residual $R = \sum\|F_o| - |F_c\|/\sum|F_o|$ to 0.081 with isotropic temperature factors, based on the data to parameter ratio of 28:1 with 102 independently varied parameters.

The function $\sum w(|F_o| - |F_c|)^2$ was minimized, where F_o and F_c are the observed and calculated structure amplitudes and *w* is the weight taken as unity for all reflections. An overall scale factor was used with a final value of 2.298 ($F_o = kF_c$). The form factors for La^{3+}, Na^+, V^{5+}, and O^{2-} were taken from the tables of McMaster et al.,[6] with real and imaginary anomalous dispersion terms given by Cromer.[7]

Table I. Final Positional and Thermal Parameters for $Na_3La(VO_4)_2$

Atom	x^a	y	z	B, Å^2
La(1)	0.4362 (4)	0.1358 (1)	0.0000	1.14 (1)
La(2)	0.0642 (4)	0.1144 (1)	0.2284 (1)	1.13 (1)
V(1)	0.5295 (8)	0.0205 (4)	0.1503 (3)	0.94 (3)
V(2)	−0.0392 (8)	0.4747 (3)	0.4071 (2)	0.78 (6)
V(3)	0.5357 (9)	0.2255 (3)	0.3223 (2)	0.40 (5)
V(4)	−0.0156 (7)	0.2296 (3)	0.0792 (3)	0.31 (5)
Na(1)	0.0127 (14)	0.3605 (13)	0.2552 (10)	2.05 (34)
Na(2)	0.5040 (18)	0.1182 (9)	0.4781 (7)	0.63 (11)
Na(3)	0.0138 (21)	0.4507 (11)	0.0757 (9)	1.07 (22)
Na(4)	0.5247 (24)	0.2995 (13)	0.1599 (9)	2.14 (30)
Na(5)	−0.0226 (25)	0.2159 (13)	0.4188 (9)	2.19 (31)
Na(6)	0.4568 (26)	0.4667 (11)	0.3151 (8)	1.90 (23)
O(1)	0.4678 (32)	0.4848 (19)	0.0665 (13)	1.54 (29)
O(2)	0.4859 (31)	0.1405 (11)	0.1494 (8)	0.67 (15)
O(3)	0.2089 (37)	0.4901 (19)	0.1868 (13)	2.31 (29)
O(4)	0.7118 (29)	0.4650 (14)	0.1922 (10)	1.38 (28)
O(5)	−0.0148 (30)	0.2613 (16)	0.1634 (11)	0.92 (20)
O(6)	0.0489 (37)	0.1183 (19)	0.0736 (13)	2.35 (29)
O(7)	0.7133 (34)	0.2556 (18)	0.0444 (13)	2.20 (27)
O(8)	0.2004 (29)	0.2830 (14)	0.0348 (10)	1.38 (25)
O(9)	0.4014 (32)	0.1175 (13)	0.3093 (11)	1.36 (24)
O(10)	0.5289 (32)	0.2565 (16)	0.4091 (13)	2.32 (28)
O(11)	0.4107 (37)	0.3089 (17)	0.2766 (12)	2.41 (29)
O(12)	0.8486 (27)	0.2197 (13)	0.3020 (10)	1.22 (20)
O(13)	0.1082 (32)	0.3736 (14)	0.4264 (11)	1.68 (28)
O(14)	0.0124 (26)	0.4961 (10)	0.3221 (7)	0.65 (14)
O(15)	0.8984 (28)	0.0567 (12)	0.4572 (10)	1.47 (23)
O(16)	0.6641 (28)	0.4660 (14)	0.4219 (10)	1.51 (24)

[a] Standard deviations are given in parentheses here and in subsequent tables.

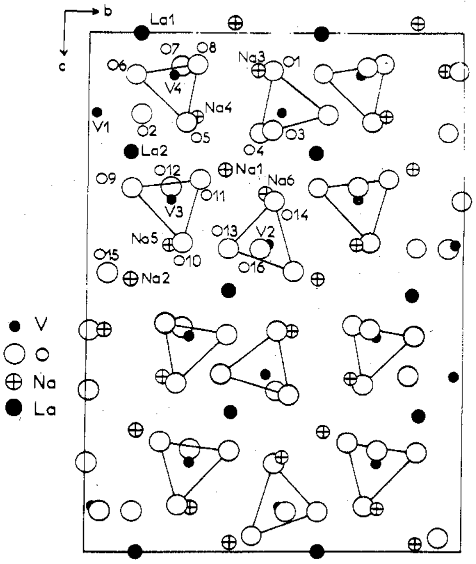

Figure 1. Projection of the structure of $Na_3La(VO_4)_2$ on the (100) plane.

The final atomic and thermal parameters are given in Table I. Table II lists the interatomic bond distances and angles and their errors.

Results and Discussion

Projections of the structure on the (100) and (010) planes are shown in Figures 1 and 2, respectively. In a simple way the structure of $Na_3La(VO_4)_2$ can be described as being an ordered superstructure of β-K_2SO_4 made up of rows, parallel to the $\vec{b}$ axis, either of alternating sodium and lanthanum atoms or of sodium atoms and vanadate tetrahedra. This particular ordered arrangement produces a doubling of the *a* and *c* parameters of the β-K_2SO_4 cell. We may thus write $a_{Na_3La(VO_4)_2} \simeq b_{K_2SO_4}$, $b_{Na_3La(VO_4)_2} \simeq 2a_{K_2SO_4}$, and $c_{Na_3La(VO_4)_2}$

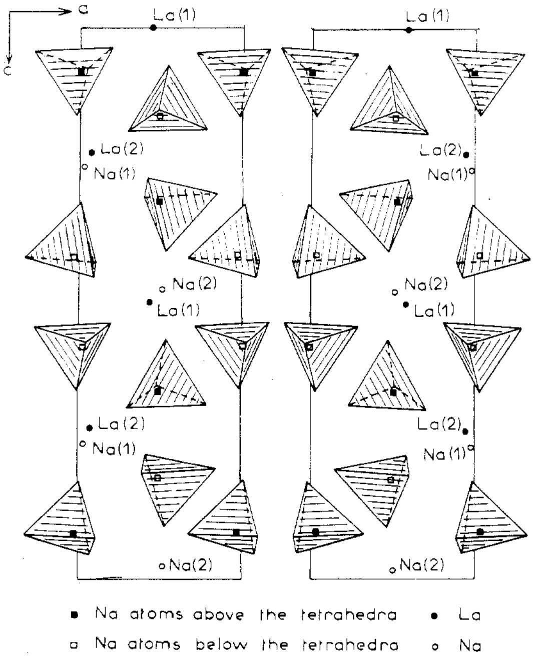

Figure 2. Projection of two different slabs of the structure on the (010) plane.

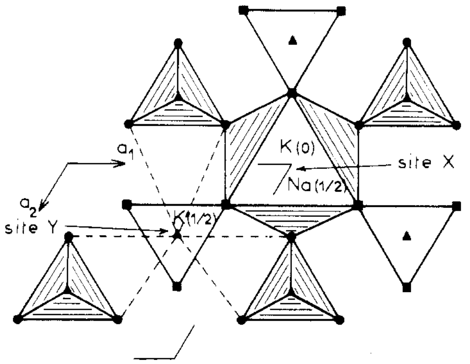

Figure 3. The glaserite structure shown as a polyhedral diagram. Oxygen atoms having the same symbol are on the same level.

$\simeq 2c_{K_2SO_4}$. Although the relationship between the $Na_3La(VO_4)_2$ and the β-K_2SO_4 atomic arrangements can be easily established, a more generalized approach will be much more valuable in the description of the structure of $A_xB_y(TO_4)_{(x+y)/2}$ type compounds. The fact that most of the sulfate, orthosilicate, and orthovanadate compounds possess structures made up of lone tetrahedra linked only by cations, as well as a profound pseudohexagonal symmetry, suggests a more topological approach.[8,9]

Glaserite $K_3Na(SO_4)_2$ and the structurally similar aphthitalite $K_2Na_2(SO_4)_2$ have a simple atomic arrangement whose hexagonal geometry defines the substructure observed in other compounds of this type such as $Ca_3Mg(SiO_4)_2$, α-Ca_2SiO_4, β-Ca_2SiO_4, and β-K_2SO_4. This structure can thus be used as an ideal model in the establishment of structural interrelationships among these compounds.

The structure of glaserite investigated by Gossner[10] and later by Fischmeister[11] is shown in Figure 3. Two large cationic sites appear in this structure. In a large ideally twelve-coordinated polyhedron six oxygen atoms make up a trigonal antiprism and six additional meridional anions constitute a hexagonal ring around this antiprism with ideal symmetry $\bar{3}2/m$ (Figure 4a). The trigonal antiprism found inside the twelve-coordinated polyhedron is in itself an octahedral site. The arrangement of the tetrahedra around this octahedron defines a "pinwheel" where the apical oxygen atoms point either up or down. A second large cation polyhedron is ideally ten-coordinated with $3m$ symmetry; again, six anions are found on the vertices of a meridional hexagon, three above share the tetrahedral base, and one below is a tetrahedral apex (Figure 4b).

Condensation of the above-mentioned pinwheels can lead to a hexagonal close-packed sheet shown in Figure 5. A comparison of this geometrically idealized structure with the actual structure shown in Figure 2 reveals a close relationship and corroborates the pseudohexagonal character of Na$_3$-

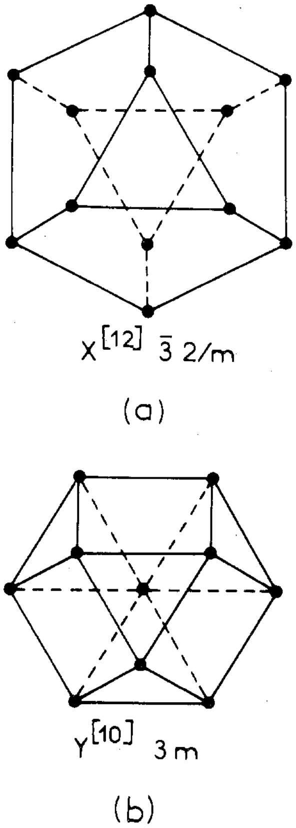

Figure 4. Idealized coordination polyhedra found in $Na_3La(VO_4)_2$.

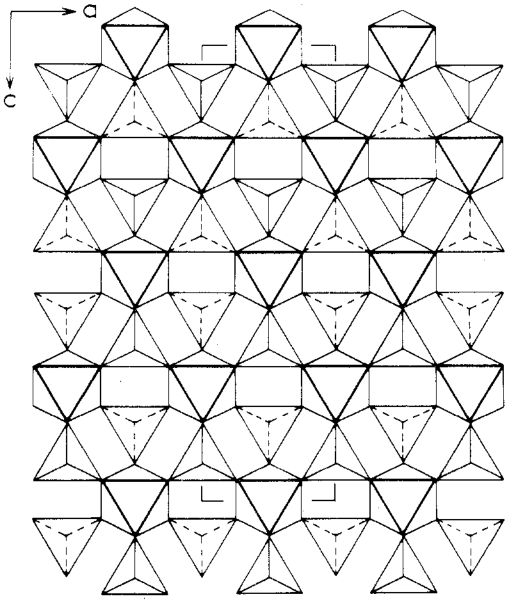

Figure 5. Condensation of "pinwheels" corresponding to an idealized sheet of the $Na_3La(VO_4)_2$ structure. The actual cell is outlined.

Table II. Bond Distances (Å) and Angles (deg)[a]

Distances

V(1a)–O(1i)	1.705 (6)	V(2)–O(13d)	1.700 (5)	V(3)–O(9)	1.730 (5)	V(4)–O(5)	1.697 (5)
V(1)–O(2)	1.724 (5)	V(2)–O(14d)	1.702 (5)	V(3)–O(10)	1.743 (5)	V(4)–O(6d)	1.629 (5)
V(1a)–O(3i)	1.681 (6)	V(2)–O(15g)	1.711 (5)	V(3)–O(11)	1.639 (5)	V(4)–O(7)	1.699 (5)
V(1a)–O(4f)	1.761 (6)	V(2)–O(16)	1.686 (5)	V(3)–O(12)	1.792 (5)	V(4)–O(8d)	1.665 (5)
⟨V(1)–O⟩	1.718 (6)	⟨V(2)–O⟩	1.700 (5)	⟨V(3)–O⟩	1.726 (5)	⟨V(4)–O⟩	1.673

Na(1)–O(3)	2.523 (9)	Na(2)–O(1b)	2.267 (9)	Na(3)–O(1)	2.586 (9)
Na(1a)–O(4e)	2.556 (9)	Na(2)–O(7b)	2.499 (9)	Na(3)–O(3)	2.481 (9)
Na(1a)–O(5e)	2.279 (9)	Na(2)–O(8b)	2.462 (9)	Na(3)–O(4e)	2.829 (9)
Na(1)–O(11)	2.376 (9)	Na(2)–O(10)	2.386 (9)	Na(3a)–O(6h)	2.412 (9)
Na(1a)–O(12e)	2.384 (9)	Na(2)–O(15)	2.405 (9)	Na(3a)–O(8)	2.725 (9)
Na(1)–O(14)	2.328 (9)	Na(2a)–O(16f)	2.603 (9)	Na(3a)–O(15g)	2.393 (9)
⟨Na(1)–O⟩	2.408 (9)	⟨Na(2)–O⟩	2.437 (9)	⟨Na(3)–O⟩	2.571 (9)

Na(4)–O(2)	2.284 (9)	Na(5)–O(7b)	2.879 (9)	Na(6)–O(3)	2.869 (9)
Na(4)–O(4)	2.654 (9)	Na(5)–O(8h)	2.574 (9)	Na(6)–O(4)	2.778 (9)
Na(4)–O(5)	2.628 (9)	Na(5)–O(10)	2.576 (9)	Na(6)–O(9c)	2.291 (9)
Na(4)–O(7)	2.556 (9)	Na(5)–O(12)	2.379 (9)	Na(6)–O(11)	2.382 (9)
Na(4)–O(8)	3.039 (9)	Na(5)–O(13d)	2.367 (9)	Na(6)–O(14)	2.520 (9)
Na(4)–O(11)	2.357 (9)	Na(5)–O(15)	2.427 (9)	Na(6)–O(16)	2.375 (9)
⟨Na(4)–O⟩	2.586 (9)	⟨Na(5)–O⟩	2.534 (9)	⟨Na(6)–O⟩	2.536 (9)

La(1a)–O(1i)	2.566 (3)	La(1)–O(8)	2.565 (2)	La(2)–O(2)	2.834 (2)	La(2)–O(6)	3.007 (3)
La(1)–O(2)	2.916 (2)	La(1a)–O(10c)	2.395 (3)	La(2a)–O(3j)	2.472 (3)	La(2)–O(9)	2.452 (3)
La(1)–O(6)	2.604 (3)	La(1a)–O(13c)	2.326 (3)	La(2a)–O(4f)	2.565 (3)	La(2a)–O(12e)	2.397 (3)
La(1)–O(7)	2.459 (3)	La(1a)–O(16c)	2.454 (2)	La(2a)–O(5e)	2.483 (3)	La(2a)–O(14j)	2.517 (2)
		⟨La(1)–O⟩	2.536 (3)			⟨La(2)–O⟩	2.591 (3)

O(1)–O(2c)	2.753 (9)	O(5)–O(7)	2.766 (9)	O(9a)–O(14j)	2.895 (9)
O(1)–O(3)	2.748 (9)	O(5)–O(8d)	2.788 (9)	O(10)–O(11)	2.759 (9)
O(1)–O(4)	2.810 (9)	O(5)–O(12)	2.860 (9)	O(10)–O(12)	2.790 (9)
O(2)–O(6)	2.867 (9)	O(6)–O(8)	2.604 (9)	O(10)–O(13)	2.900 (9)
O(2)–O(7)	2.909 (9)	O(6a)–O(7e)	2.766 (9)	O(11)–O(12)	2.798 (9)
O(2a)–O(3i)	2.832 (9)	O(6a)–O(13c)	2.880 (9)	O(13)–O(14)	2.726 (9)
O(2a)–O(4f)	2.855 (9)	O(7)–O(8)	2.895 (9)	O(13)–O(15c)	2.674 (9)
O(3)–O(4)	2.832 (9)	O(7b)–O(8h)	2.753 (9)	O(13a)–O(16e)	2.807 (9)
O(3)–O(14)	2.848 (9)	O(7a)–O(10c)	2.826 (9)	O(14)–O(15c)	2.805 (9)
O(3)–O(4e)	2.799 (9)	O(9)–O(10)	2.862 (9)	O(14a)–O(16e)	2.777 (9)
O(5)–O(6d)	2.704 (9)	O(9)–O(11)	2.799 (9)	O(15b)–O(16e)	2.846 (9)
		O(9)–O(12)	2.893 (9)	⟨O–O⟩	2.800 (9)

Angles

O(1)–V(1)–O(2)	107.0 (3)	O(9)–V(3)–O(10)	111.0 (3)
O(1)–V(1)–O(3)	106.2 (3)	O(9)–V(3)–O(11)	112.3 (3)
O(1)–V(1)–O(4)	110.2 (3)	O(9)–V(3)–O(12)	110.5 (3)
O(2)–V(1)–O(3)	110.4 (3)	O(10)–V(3)–O(11)	109.3 (3)
O(2)–V(1)–O(4)	112.3 (3)	O(10)–V(3)–O(12)	104.2 (3)
O(3)–V(1)–O(4)	110.4 (3)	O(11)–V(3)–O(12)	109.2 (3)
O(13)–V(2)–O(14)	106.5 (3)	O(5)–V(4)–O(6)	108.8 (3)
O(13)–V(2)–O(15)	103.3 (3)	O(5)–V(4)–O(7)	109.1 (3)
O(13)–V(2)–O(16)	112.0 (3)	O(5)–V(4)–O(8)	112.1 (3)
O(14)–V(2)–O(15)	110.6 (3)	O(6)–V(4)–O(7)	112.5 (3)
O(14)–V(2)–O(16)	110.2 (3)	O(6)–V(4)–O(7)	104.5 (3)
O(15)–V(2)–O(16)	113.8 (3)	O(7)–V(4)–O(8)	109.9 (3)
		⟨O–V–O⟩	109.4 (3)

[a] Symmetry transformations: (a) $\bar{x}, \bar{y}, {}^1/_2 + z$; (b) $x, {}^1/_2 - y, {}^1/_2 + z$; (c) $\bar{x}, {}^1/_2 + y, z$; (d) $1 + x, y, z$; (e) $1 + x, 1 + y, z$; (f) $x, 1 + y, 1 + z$; (g) $1 + x, 1 + y, 1 + z$; (h) $1 + x, {}^1/_2 - y, {}^1/_2 + z$; (i) $x, {}^3/_2 - y, {}^1/_2 + z$; (j) $1 + x, {}^3/_2 - y, {}^1/_2 + z$.

$La(VO_4)_2$. The pseudohexagonal cell parameters for $Na_3La(VO_4)_2$ are $a_H = 5.58$ Å, $b_H = 5.51$ Å, and $c_H = 7.12$ Å, while for glaserite they are $a = 5.65$ Å and $c = 7.29$ Å. We can thus say that the structure of $Na_3La(VO_4)_2$ is a distorted variation of the glaserite structure and can be derived from a corresponding condensation of idealized pinwheels.

Furthermore, the $Na_3La(VO_4)_2$ structure seems to be geometrically related to the merwinite structure [$Ca_3Mg(SiO_4)_2$: $a = 13.25$ Å, $b = 5.29$ Å, $c = 9.33$ Å, $\beta = 91.90°$, $P2_1/a$] which has been shown to be a distorted glaserite structure.[8]

Ideally in this structure four different types of polyhedra can be expected: a tetrahedron TO_4, a twelve-coordinated polyhedron $X^{[12-p]}$ with $p = 0$ and an octahedron $M^{[6]}$ ($X^{[12-p]}$ with $p = 6$), both having a common center (Figures 3 and 5), and finally a ten-coordinated polyhedron $Y^{[10]}$ with its center above or below the tetrahedra (Figures 3 and 5). Actual structural distortion, due to the need for these sites to accommodate cations of different size and charge, leads to lower coordination numbers as is observed in most of these compounds.

In $Na_3La(VO_4)_2$ all of the above sites are occupied, but with lower coordination for X and Y. We have thus a network of isolated vanadate tetrahedra forming the skeleton of this structure. The atoms La(1) and La(2) occupy the X sites with eight-coordination, and Na(1) and Na(2), the central M octahedra with six-coordination, while Na(3), Na(4), Na(5), and Na(6) occupy the Y sites with six-coordination. The actual formula can be written as $X^{[8]}{}_2Y^{[6]}{}_4M^{[6]}{}_2[TO_4]_4$ as compared to the geometrical ideal of $X^{[12]}{}_2Y^{[10]}{}_4M^{[6]}{}_2[TO_4]_4$, where X = La, Y = Na, and M = Na.

The occupation of the different sites by the various atoms is in accordance with the observations of Moore[9] for a number of similar compounds. When two different cations are present, with different crystal radii, in the $X^{[12-p]}$ sites, the larger cation will have p small and the smaller cation will have p large. We therefore have lanthanum in X with p equal to 4 and sodium in M ($X^{[12-p]}$, $p = 6$). When two cations of different charges are present, the lower charged ion will preferentially occupy the Y polyhedron (La^{3+} in X, Na^+ in Y).

The average V–O distances in the four independent tetrahedra, 1.718, 1.700, 1.726, and 1.673 Å, respectively (Table II), are within the V–O distances reported recently by Robertson and Kostiner[12] in $FeVO_4$ (V–O = 1.660–1.806 Å) and by Gopal and Calvo[13] in $Ca_3(VO_4)_2$ (⟨V–O⟩ = 1.691, 1.701, and 1.694 Å for three independent tetrahedra). The average Na–O distances (Table II) fall into two categories: two short distances for Na(1) and Na(2)—2.408 and 2.437 Å, respectively—and four long distances for Na(3), Na(4), Na(5), and Na(6)—2.571, 2.586, 2.534, and 2.536 Å, respectively. These two different types of distances can be easily explained by the fact that the sodium atoms are present in two different sites. Atoms Na(1) and Na(2) are found in trigonal-antiprismal sites (octahedra) with very little cation–cation repulsion since the X polyhedra share faces only with other large X polyhedra. We have thus normal Na–O bonds. Sodium–oxygen bonds of similar length (2.418 Å) have been found by Durand et al.[14] in $K_3Na(PO_3F)_2$, where the sodium atom is in an equivalent position. Atoms Na(3) to Na(6) occupy the Y site, where there exists severe cation–cation repulsion between this polyhedron and the highly charged tetrahedron with which it shares a face. We can therefore expect much longer bonds.

The La–O distances all fall within values reported for $La_2Ti_2O_7$ (2.38–3.09 Å) by Gasperin[15] and for La_2MoO_6 (2.33–2.38 Å) by Sillén and Lundborg.[16] No La–La distances were found corresponding to significant bonding.

All O–O distances are normal with an average oxygen–oxygen distance of 2.800 Å. The individual O–V–O angles in the different tetrahedra are slightly distorted as expected, but the average tetrahedral angle of 109.4° is very normal.

In conclusion, in structures which are made up of isolated TX_4 tetrahedra, we observe that these tetrahedra can arrange themselves in a variety of ways by simply rotating around their centers and condensing themselves in "pinwheels" in such a way that they can accomodate in their network a number of different cations with different coordinations. This explains the fact that we find such compounds as β-K_2SO_4 and $K_3Na(PO_3F)_2$ to be topologically related.

Registry No. $Na_3La(VO_4)_2$, 55859-79-5.

Supplementary Material Available: A listing of structure factor amplitudes (17 pages). Ordering information is given on any current masthead page.

References and Notes

(1) J. A. Baglio and G. Gashurov, *Acta Crystallogr., Sect. B*, **24**, 292 (1968).
(2) E. Patscheke, H. Fuess, and G. Will, *Chem. Phys. Lett.*, **2**, 47 (1968).
(3) G. Blasse, and A. Brill, *Philips Tech. Rev.*, **31**, 324 (1970).
(4) G. Le Flem and R. Olazcuaga, *Bull. Soc. Chim. Fr.*, **7**, 2769 (1968).
(5) R. Salmon, C. Parent, A. Berrada, R. Brochu, A. Daoudi, M. Vlasse, and G. Le Flem, *C. R. Hebd. Seances Acad. Sci.*, **280**, 805 (1975).
(6) W. H. McMaster, N. Kerr del Grande, J. H. Mallet, and J. H. Hubbel, "Compilation of X-ray Cross Sections", Report UCRL-50174, National Bureau of Standards, 1969, Section II, Revision 1.
(7) D. T. Cromer, *Acta Crystallogr., Sect. B*, **18**, 17 (1965).
(8) P. B. Moore, and T. Araki, *Am. Mineral.*, **57**, 1355 (1972).
(9) P. B. Moore, *Am. Mineral.*, **58**, 32 (1973).
(10) B. Gossner, *Neues Jahrb. Mineral., Geol. Palaeontol., Abh. Abt. A*, **57**, 89 (1928).
(11) H. F. Fischmeister, *Monatsh. Chem.*, **93**, 420 (1962).
(12) B. Robertson and E. Kostiner, *J. Solid State Chem.*, **4**, 29 (1972).
(13) R. Gopal and C. Calvo, *Z. Kristallogr., Kristallgeom., Kristallphys., Kristallchem.*, **137**, 67 (1973).
(14) J. Durand, W. Granier, L. Cot, and J. L. Galigne, *Acta Crystallogr., Sect. B*, **31**, 1533 (1975).
(15) M. Gasperin, *Acta Crystallogr., Sect. B*, **31**, 2129 (1975).
(16) L. G. Sillén and K. Lundborg, *Z. Anorg. Chem.*, **252**, 2 (1943).

Contribution from the School of Chemistry, Rutgers University,
New Brunswick, New Jersey 08903

Crystal Structure and Magnetic Properties of Copper Citrate Dihydrate, $Cu_2C_6H_4O_7 \cdot 2H_2O$

DONALD MASTROPAOLO, DANA A. POWERS, JOSEPH A. POTENZA,* and HARVEY J. SCHUGAR*

Received January 21, 1976 AIC60050M

The crystal and molecular structure of copper citrate dihydrate, $Cu_2C_6H_4O_7 \cdot 2H_2O$, has been determined from single-crystal three-dimensional x-ray data collected by counter methods. The compound crystallizes as green six-sided plates in space group $P2_1/a$ (C_{2h}^5, No. 14) with $Z = 4$, $a = 14.477$ (9) Å, $b = 9.718$ (6) Å, $c = 6.890$ (5) Å, $\beta = 91.27$ (5)°, $d_{calcd} = 2.413$ g/cm³, and $d_{obsd} = 2.39$ (1) g/cm³. Least-squares refinement of 1172 reflections having $F^2 \geq 3\sigma$ gave a conventional R factor of 0.079. There are no discrete molecules in the crystal; it consists of a three-dimensional array of Cu(II) ions linked by alkoxo and three types of carboxylate bridges. The asymmetric unit contains two H_2O molecules, one heptadentate $C_6H_4O_7^{4-}$ citrate ligand, and two crystallographically unique Cu(II) ions with O_5 ligand sets. An alkoxo and a syn–syn carboxylate group bridge the Cu(II) ions within this unit. An anti–syn carboxylate group joins these units into zigzag chains, which in turn are joined by a second type of anti–syn carboxylate bridge to form the three-dimensional network. The complex does not exhibit the electronic absorption at ~380 nm which is characteristic of strongly coupled Cu(II) dimers. Its magnetism follows the Curie–Weiss law [$\chi \propto 1/(T - \Theta)$], with Θ falling in the +24–+40 K range. An unusual twisting of the Cu(II) coordination spheres within the asymmetric unit apparently suppresses the strong antiferromagnetism typically observed with alkoxo and syn–syn carboxylate bridged Cu(II) complexes.

The aqueous copper(II) citrate system has been studied extensively,[1] and several polynuclear species have been identified. A dimeric copper(II) citrate complex of possible composition $[Cu_2(OH)_2(C_6H_5O_7)_2]^{4-}$ has been characterized in solution, while, from a different sample, a Cu–Cu distance of 3.1 Å was deduced from a detailed ESR analysis.[1] Both magnetic susceptibility and ESR data indicated essentially no spin–spin coupling between Cu(II) ions. This result appeared odd to us at first because substantial antiferromagnetic interactions usually are observed between Cu(II) ions bridged presumably by ligands such as OH, alkoxo, and carboxylate (all available in the citrate system). However, recent studies of a series of $Cu_2(OH)_2^{2+}$ species have shown that the extent and nature of magnetic coupling (antiferromagnetic or fer-